Research Article

Yongsen Niu, Boren Xu, Xin Yi, Xi Wang*, and Chunwang Yi*

A green and facile synthesis route of nanosize cupric oxide at room temperature

https://doi.org/10.1515/ntrev-2024-0070
received October 24, 2023; accepted July 10, 2024

Abstract: Heat, ultrasonic, microwave, and external energy are the essential conditions in the conventional preparation of nano-cupric oxide (CuO) from copper hydroxide ($Cu(OH)_2$) precursor. In this work, $CuSO_4$ aqueous solution (0.02 mol) was gradually added dropwise into the methanol/sodium hydroxide ($NaOH/CH_3OH$) solution (0.04 mol) in 20 min at normal temperature and then constantly stirred the black solution for about 5 min; nano-CuO was synthesized. The as-prepared CuO had a high purity and a regular nanosize of 4–10 nm. What is more, the by-product sodium sulfate (Na_2SO_4) could be separated using a high-speed centrifuge, indicating that the methanol could be conveniently recycled; thereby, an environmentally friendly sustainable route of the preparation of nano-CuO was developed. In addition, the as-prepared nano-CuO was melt-compounded with polyamide 6 to produce fiber composites. The results showed that the nano-CuO was uniformly dispersed in PA6 fiber composites and presented an excellent antibacterial performance. Most importantly, the function of methanol in the dehydration process was revealed.

Keywords: nano-CuO, green synthesis, controllable size, methanol recycle, antibacterial

1 Introduction

Copper oxide (CuO), as an important metal oxide, has gained an ever-increasing interest and a wide range of applications [1–5]. Except for the common use in rayon, stained glass, and ceramics [6–10], it also has been widely used in antifouling paints for boats, inks, and antimicrobial coatings [11,12]. In addition, CuO nanocrystalline particle is the basis of some high-Tc superconductors, thereby attracting much attention in magnetic storage media, solar energy transformation, electronics, and catalysis [13–16].

Traditionally, physical gas phase synthesis and chemical low-temperature hydrothermal solution method are commonly used for the growth of CuO nanostructure assemblies [17–19]. However, the commercial potential of gas phase-grown CuO nanostructures was restricted owing to the high investment for equipment, as well as the high-energy consumption [13]. Compared with the physical technique method, chemical techniques exhibit indisputable advantages, because the chemical techniques can produce CuO with high purity and small particle size with lower energy consumption and costs. Over the years, various chemical techniques, such as hydrothermal method [20–22], sol–gel method [23], sonochemical method [24,25], microwave [26], and so on methods, were explored to prepare CuO. Howbeit, a number of studies have disclosed that to impel the copper hydroxide ($Cu(OH)_2$) precursor to transform into CuO via chemical methods, an external driving force, such as heat, ultrasonic, and microwave, was essential.

As is known to all of our knowledge, there lacks study focused on the one-pot preparation of CuO at room temperature using convenient facilities [27]. Some researchers claimed to notice that, given a long enough time, $Cu(OH)_2$ could partially transform into CuO at room temperature [28,29]. Cudennec *et al.* reported that in the presence of hydroxide ions (OH^-), the mentioned transformation would become very fast, for the reason that the divalent copper ions were dissolved under the form of tetrahy-droxocuprate(II) anions ($Cu(OH)_4^{2-}$) [30]. Later, Zhao and Zhao further developed the method to produce CuO at room temperature using $Cu(OA)_2$

* **Corresponding author: Xi Wang,** National & Local Joint Engineering Lab. for New Petro-chemical Materials and Fine Utilization of Resources, Hunan Normal University, Changsha, Hunan, 410081, China, e-mail: wangxiiccas@hotmail.com
* **Corresponding author: Chunwang Yi,** National & Local Joint Engineering Lab. for New Petro-chemical Materials and Fine Utilization of Resources, Hunan Normal University, Changsha, Hunan, 410081, China, e-mail: cwyi@hunnu.edu.cn
Yongsen Niu, Boren Xu, Xin Yi: National & Local Joint Engineering Lab. for New Petro-chemical Materials and Fine Utilization of Resources, Hunan Normal University, Changsha, Hunan, 410081, China

precipitates prepared by the reaction of sodium oleate and copper sulfate as precursors [31].

As well as known, it took at least 3 h to obtain CuO at room temperature using the conventional synthesis methods. Besides, few individuals are concerned about the recycle of the solvent used in the preparation of CuO. Herein, in this work, we report a novel chemical method for the preparation of CuO nanoparticles by simply adding copper sulfate ($CuSO_4$) aqueous solution into methanol/sodium hydroxide (CH_3OH/NaOH) solution. By this means, CuO particles with regular nanosize could be obtained conveniently in one step at room temperature in 20–30 min, which significantly reduced the preparation time compared to that of the published work. What is more, the by-product sodium sulfate (Na_2SO_4) could be separated using a high-speed centrifuge, which allowed the recovery and repeated circle of methanol to be realized, so that a sustainable method for preparing nano-CuO was proposed. In addition, the as-prepared CuO was then blended with polymer to produce antibacterial fiber composites. The results referred that the composite had a superior antibacterial performance and good spinnability. Most importantly, using a high-speed centrifuge to separate the water-soluble by-product sodium sulfate from its aqueous solution will have far-reaching theoretical direction and application implications.

2 Materials and methods

2.1 Materials

Analytical grade $CuSO_4$, NaOH, and ether ($C_2H_5OC_2H_5$) were obtained from Sinopharm Chemical Reagent Co., Ltd. (Shanghai, China). Analytical grade CH_3OH was obtained from Tianjin Comeo Chemical Reagent Co., Ltd. (Tianjin, China). PA6 (η_r = 2.48, M_n = 22,500) was purchased from Xinhui Meida Nylon Chemical Co., Ltd. (China). *Escherichia coli* (TOP10) and *Staphylococcus aureus* (CMCC26003) were bought from the Guangdong Institute of Microbiology (China). The other chemical agents are analytic pure.

2.2 Methods

2.2.1 Preparation of nano-CuO

First, 1.6 g (0.04 mol) of NaOH was dissolved in 100 ml of CH_3OH in a 400-ml beaker (Figure 1a). Then, 3.82 g of $CuSO_4$ (0.02 mol) was fully dissolved in 40 ml of deionized water in a 100-ml beaker (Figure 1b). Following that, the $CuSO_4$ aqueous solution was gradually added dropwise into the above-mentioned NaOH/CH_3OH solution for 20 min. Later,

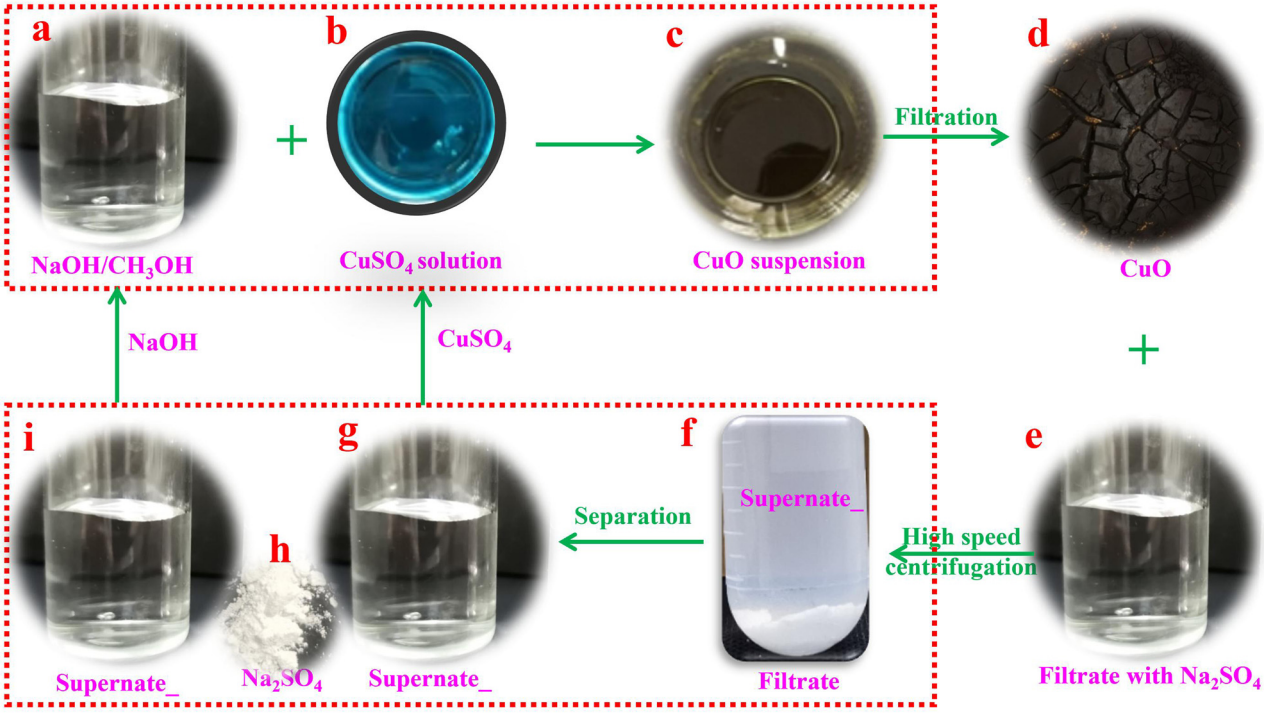

Figure 1: The preparation process of nano-CuO at room temperature and the recycle of CH_3OH.

constantly stirred the black solution at normal temperature for about 5 min to ensure the completion of the transformation (Figure 1c). After the reaction, the black suspension was filtrated to separate CuO. The as-prepared CuO (Figure 1d) was washed with deionized water and ethyl ether thrice and then dried at 50°C for 24 h in a vacuum oven.

2.2.2 Recovery of CH_3OH and cycle preparation of nano-CuO

When the above-mentioned preparation process was ended, CuO was first separated through filtration (Figure 1d and e) and then used a high-speed centrifuge to remove the by-product Na_2SO_4 under a rotating speed of 10,000 rpm (Figure 1f). Following that, the transparent CH_3OH aqueous solution was equally divided into two groups (Figure 1g and i). Afterwards, 1.6 g of NaOH was added to one of them, and 3.82 g of $CuSO_4$ was added to another group. Through duplicating the preparation process at normal temperature (Figure 1c), nano-CuO precipitates were obtained again.

2.2.3 Preparation of PA6-CuO composites and fibers

After fully dried, CuO precipitates and PA6 pellets were mixed and then melt-extruded by a co-rotating twin-screw extruder (SHJ-20, Nanjing Giant Co., China). The length and diameter of the extruder are 800 and 20 mm, respectively. The temperature for the I, II, III, IV, and V zones of the extruder was 180, 235, 235, 238, and 240°C, respectively. By varying the adding mass ratio of PA6 and nano-CuO, batches of PA6-CuO composites were produced. The concentration of Cu^{2+} in PA6 was 0, 0.12, 0.24, 0.36, and 0.6 wt%, respectively, and pure PA6 was used as a comparison.

Later, some of the selected PA6-CuO composites were further fabricated into yarns by melt-spinning with a spinning speed of 800 m/min under the temperature of 260°C.

2.2.4 Antibacterial tests

To evaluate the bactericidal activity of PA6-CuO fiber composites on *E. coli* (TOP10) and *S. aureus* (CMCC26003), the colony-forming count method was adopted, and Gram-negative and Gram-positive bacteria were used as the model, respectively. After 18–20 h of incubation, sterile phosphate buffer saline (1×) was used to serially dilute the initially cultured bacteria of *E. coli* and *S. aureus* to 1×10^6–5×10^6 CFU/ml. 5 ml of bacterial solution and 70 ml of buffer solution were subsequently poured into a conical flask in which 1 g of the as-prepared sample was previously placed. Following that, the incubation was executed in a shaking incubator at 37°C and 220 rpm for 24 h. Then, 100 µl of each bacterial suspension was spread on a Luria–Bertani (LB) solid agar plate. After incubating the agar plates in an incubator for 24 h at 37°C, the living bacterial colonies were finally counted.

2.2.5 Characterizations

A typical Fourier transform infrared spectrometer (FTIR) analysis was performed on a WQF-200 spectrometer (Beijing Second Optical Instrument Factory) using a solid potassium bromide method. The recorded range of the spectra was 4,000–400 cm^{-1}.

The particle sizes of nano-CuO particles were observed by transmission electron microscopy (TEM, 200CX, JEOL, Japan). An S-4800 field emission scanning electron microscope was used to investigate the PA6-CuO fibers' morphology, as well as the dispersion of nano-CuO in the composites, the samples were coated with conductive gold before a test.

PANalytical X'Pert Pro multipurpose powder diffractometer with nickel-filtered Cu-Ka radiation (λ = 1.54 Å) was adopted to execute the X-ray diffraction (XRD) tests conducted at 45 kV and 40 mA. The sweeping signals from 5° < 2θ < 80° were collected, and the scan rate is 2°(2θ)/min. The chemical composition was analyzed by X-ray photoelectron spectroscopy (XPS). X-ray photoelectron spectroscopy profiles were collected on a K-Alpha+ (Thermo Fisher Scientific, USA) apparatus using monochromatic Al Kα (1486.6 eV) radiation as the radiation source.

3 Results and discussion

3.1 The effect of the adding sequence on the purity of nano-CuO

Figure 2 shows the complete experimental procedures for the preparation of nano-CuO in our lab. As we all know, the reaction of equivalent $CuSO_4$ and NaOH aqueous solution produced only blue copper hydroxide ($Cu(OH)_2$) at room temperature. Blue powders were generated by adding CH_3OH into $CuSO_4$ aqueous solution. Putting solid $CuSO_4$ into CH_3OH at room temperature also produced blue powders; however, the powders were actually water-insoluble copper sulfate basic crystals with regular shape (Figure S1).

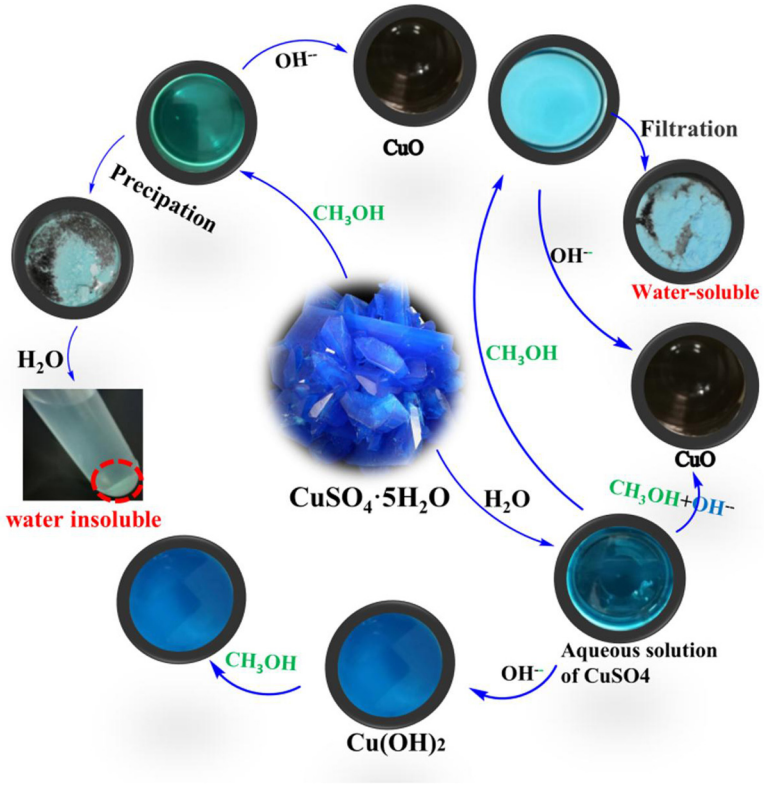

Figure 2: The complete experimental procedures in lab.

Interestingly, when $CuSO_4$ aqueous solution was added dropwise into CH_3OH/NaOH solution under room temperature, some black precipitates were produced immediately; these black precipitates were later confirmed to be nano-CuO. Adding other copper aqueous solution like copper chloride into NaOH/CH_3OH solution, or using ethanol, ethylene glycol to substitute CH_3OH, black precipitates were also obtained under room temperature (Figure S2). Moreover, using other water-soluble hydroxides instead of NaOH also achieved a similar result in this work (Figure S3). In sum, strong alkaline and adequate alcohol is in favor of the rapid preparation of CuO at room temperature.

Herein, a $CuSO_4$ aqueous solution was prepared by adding 0.02 mol of $CuSO_4$ into 40 ml of water. Then, the $CuSO_4$ aqueous solution was added to a series of NaOH/methanol solution to further investigate the generation of CuO at room temperatures. As shown in Figure 3, it is clear to see that the adding mass of NaOH and CH_3OH had a strong effect on the purity of CuO. XRD results indicated that adding equivalent $CuSO_4$ aqueous solution into NaOH aqueous solution, it only produced blue $Cu(OH)_2$ (Figure 3a). However, it tended to produce a mixture of CuO and $Cu(OH)_2$ if we added dropwise 0.02 mol of $CuSO_4$ aqueous solution into NaOH/methanol (NaOH is 0.2 and 0.3 mol in this case). Interestingly, if we repeated this process in a very short time, a green mixture of $Cu(OH)_2$ and columnar sodium copper alum ($Na_2(CuSO_4)_2{\cdot}2H_2O$) (Figure 3b and c, Figure S4) was obtained. That is, pure CuO could not be obtained under an improper molar ratio of NaOH and $CuSO_4$. When an equivalent amount of $CuSO_4$ was added dropwise into NaOH/CH_3OH solution (prepared by 0.04 mol of NaOH and 25, 50, and 100 ml of CH_3OH), pure CuO (Figure 3d–f) could be obtained at room temperature. The results inferred that except for the NaOH and methanol, the adding speed also had an influence on the generation of CuO. What is more, the variation of the reaction temperature (0–30°C) had an influence on the reaction speed; however, it did not affect the purity of nano-CuO.

3.2 Characterization of nano-CuO

The composition of the product shown in Figure 3f was analyzed by XRD and FTIR analysis. Figure 4 presents the XRD and FTIR patterns of the sample before washing. The characteristic 2θ of 32.5°, 39.0°, 48.8°, 61.6°, 66.3°, and 68.1° is assigned to the (110), (200), (−202), (−113), (−311), and (220) crystal faces, respectively, of the CuO standard map card (JCPDS file: 72-0629); the 2θ locates at 19.0°, 29.0°, 32.1°, 38.6°, 49.5°, 59.5°, and 71.4° are the characteristic peaks of Na_2SO_4

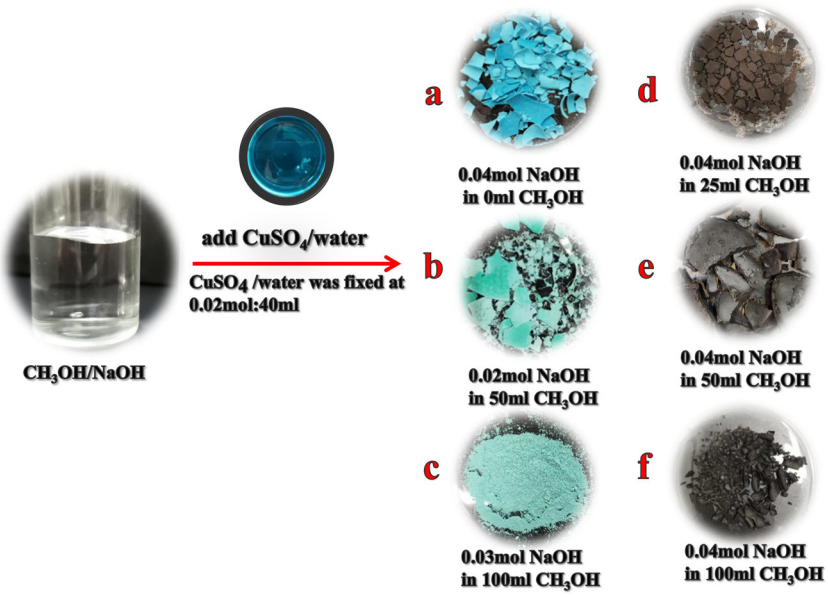

Figure 3: The effect of adding content of NaOH and CH_3OH on the purity of CuO.

(JCPDS file: 74-1738) and are assigned to the (111), (004), (131), (222), (151), (333), and (119) crystal faces, respectively. The above results show that the obtained sample is a mixture of CuO and Na_2SO_4.

Figure 4b presents the FTIR spectrum of the black precipitates. The absorption peak around 3,400 cm^{-1} is attributed to the stretching vibration of −OH, indicating the existence of hydroxyl groups. The stretching vibration peaks of $-CH_3$ correspond to 2,925 and 2,854 cm^{-1}. 1,117 cm^{-1} is the C–O stretching vibration peak of CH_3OH, and the characteristic peaks of CuO bond are located at 861, 626, and 548 cm^{-1}, respectively. The infrared analysis results show that the product contains hydroxyl, methyl, and Cu–O bonds. Therefore, we conjecture that part of the CH_3OH was absorbed on the surface of CuO.

The absorbed methanol and water-soluble Na_2SO_4 in the black precipitates were then removed by further water and ether washing. The pure black powders were further characterized by FTIR, XRD, XPS, and inductively coupled plasma optical emission spectrometer (ICP-OES). As shown in Figure 5a, the FTIR peaks at 828, 626 and 548 cm^{-1} are

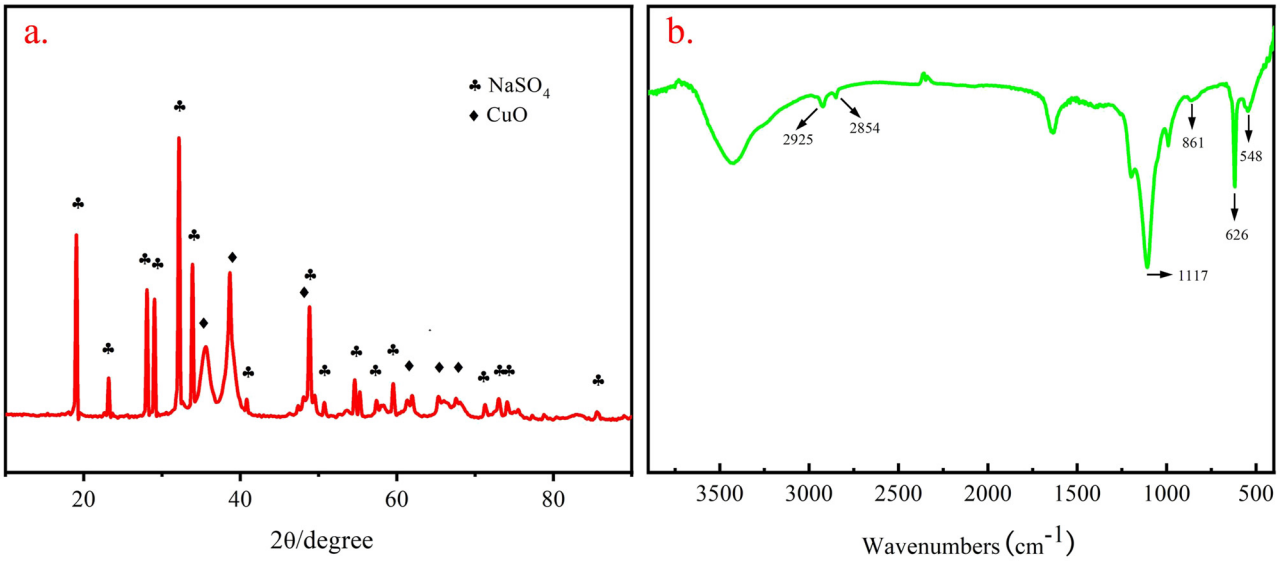

Figure 4: Characterizations of the as-prepared CuO nanoparticles before washing: (a) XRD spectra and (b) FTIR spectra.

attributed to nano-CuO. The absorption peak at 3,407 cm^{-1} is assigned to the −OH stretching vibration, owing to the absorption of water during the test. In addition, due to the large proportion of surface atoms in the nano-CuO crystals, the stretching vibration of the hanging bond on the vertical surface became very active, resulting in a sharp characteristic peak at 1,550 cm^{-1}. Changing the adding sequence could result in an incomplete reaction and leave some $Cu(OH)_2$ in CuO, multi −OH stretching vibrations were observed around 3,500 cm^{-1} (Figure S4).

The XRD pattern of the black powders after water and ether washing is presented in Figure 5b. The intensities and positions of the peaks are in good agreement with the values of the literature and the data from JCPDS file: 72-0629 [19,26]. Based on the diffraction peaks, the as-prepared CuO can be indexed to the single-phase CuO with a monoclinic structure. What is more, the broadening of all recorded peaks in the XPS spectrum indicates that there were nanoscale crystallites existed in the structure [19]. In addition, XRD results prove that there are no other impurities in the as-prepared CuO. The average size of the CuO nanoparticles was further calculated according to the Debye–Scherer formula, which is about 6 nm.

The phase purity and chemical composition of the black powders were further investigated by XPS. The CuLm2 scan curve (Figure 5c) indicates that there is a peak of 569.4 eV, which proves that there is only Cu(II) in the products. Furthermore, the peaks at 932.2 and 952.9 eV in Figure 5d are attributed to the Cu2p3/2 and Cu2p1/2, respectively. In addition, the satellite peaks are also produced by Cu^{2+}. In Figure 5f, there are two O1s peaks in the O1s core-level spectrum: the one at 530 eV is in agreement with O^{2-} in CuO and another one at 531.6 eV is attributed to O adsorbed on the surface of the rectangular-shaped structure of CuO [32–34]. As shown in Figure 5e, the wide survey scan spectrum of the sample presents only CuO and C peaks. Thus, XPS results proved that the sample was composed of CuO. The ICP-OES result further proved that the content of Cu^{2+} was 79.67%, which is essentially consistent with the theoretic content in pure CuO.

TEM results show that the CuO particles have a regular nanosize. The average length and thickness of the particles are around 20 and 5 nm, respectively, which is highly consistent with the result calculated by the Debye–Scherer formula (Figure 6a–c). Further, a high-resolution transmission electron microscope indicates the main crystal surface (111) of CuO, and the spacing of the lattice fringe is 0.215 nm (Figure 6d, Figure S5). Obviously, the size of the as-prepared CuO particles is significantly smaller than that of the nanoleaves with lengths of 500 nm and widths of 200 nm synthesized by a similar method [31].

Combined with the results of the upper experiments, we denote that by simply dropping $CuSO_4$ into CH_3OH/NaOH solution in a suitable ratio, pure nano-CuO could be obtained under room temperature in short time.

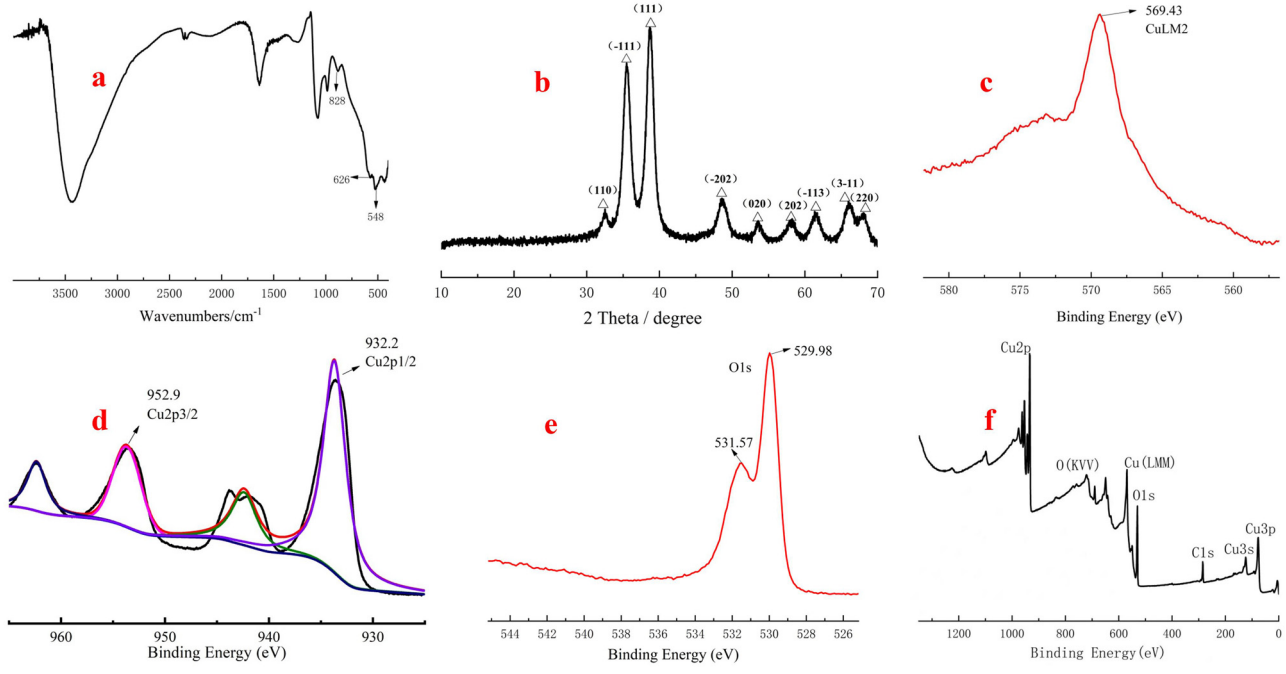

Figure 5: Characterizations of as-prepared CuO nanoparticles after washing: (a) FTIR pattern and (b) XRD pattern; high-resolution XPS spectra of (c) Cu LMM2 and (d) Cu2p, and (e) O1s; and (f) wide X-ray photoelectron spectra.

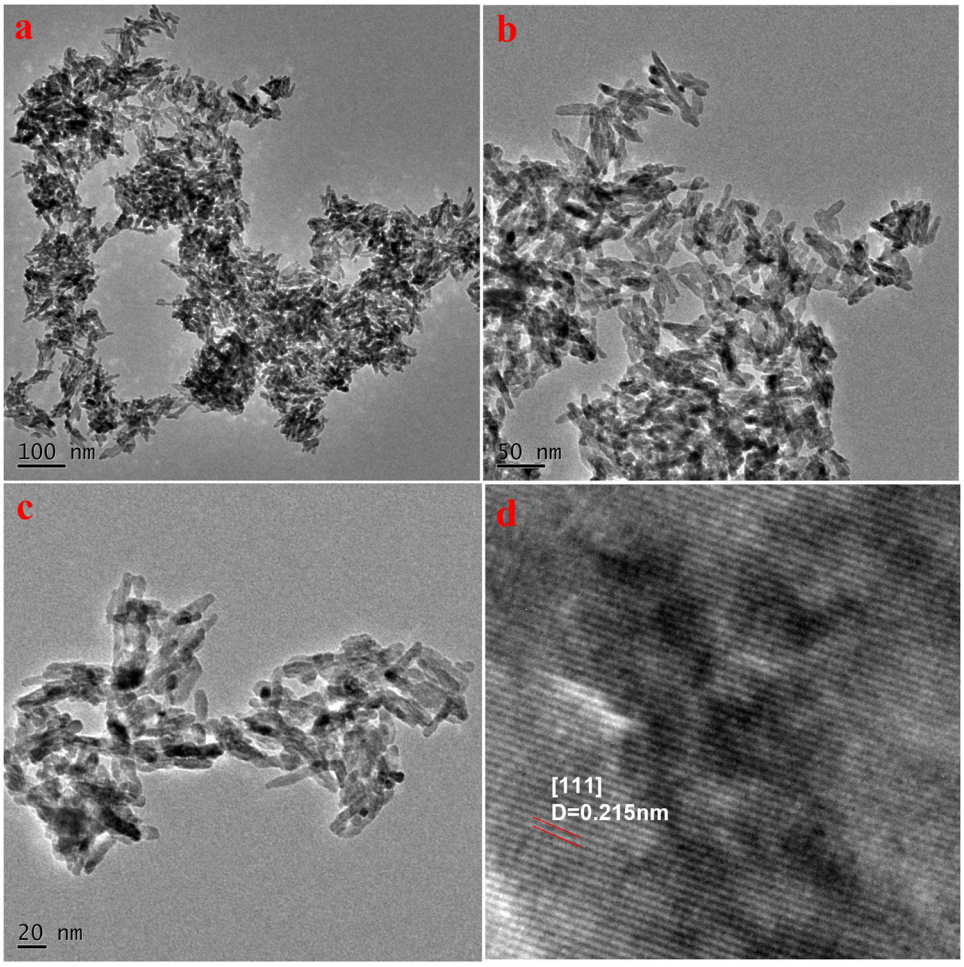

Figure 6: TEM (a–c) and HTEM (d) images of the as-prepared CuO nanoparticles.

3.3 Presumable mechanism of preparation of CuO

Cudennec *et al.* proposed a probable mechanism for the transformation of $Cu(OH)_2$ to CuO in an alkaline solution, but they neglected the dehydration step of $Cu(OH)_4^{2-}$ which is of great importance to promote the transformation. Besides, they did not discuss how to promote the dehydration process. In this case, we further developed the probable mechanism as summarized below (Figure 7): when $CuSO_4$ was added dropwise into $NaOH/CH_3OH$ solution, it produced a small amount of $Cu(OH)_2$ and Na_2SO_4 (step I). The tiny amount of $Cu(OH)_2$ then quickly transformed to an unstable $Cu(OH)_4^{2-}$ due to there being an excess of OH− (step II). Following that, the unstable $Cu(OH)_4^{2-}$ triggered an equilibrium reaction to generate CuO and water (step III). Finally, the minute quantities of the released water were rapidly absorbed by CH_3OH (step IV and Figure 8a), which further promoted the dehydration of $Cu(OH)_4^{2-}$ to produce CuO.

In the process of dropping, with the addition of $CuSO_4$ aqueous solution, the transparent $NaOH/CH_3OH$ solution became turquoise and then turned blackish green $Cu(OH)_4^{2-}$ to black (CuO), which can be regarded as additional evidence of the transformation. Thereby, we claim that the strong alkaline condition allows the formation of $Cu(OH)_4^{2-}$ in this one-pot synthesis route, while the excessive CH_3OH plays a key role as a dehydrating agent of $Cu(OH)_4^{2-}$.

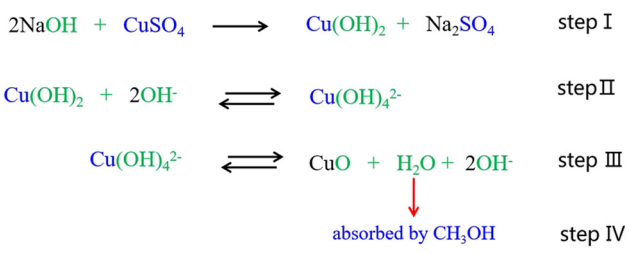

Figure 7: Possible mechanism for preparation of nano-CuO.

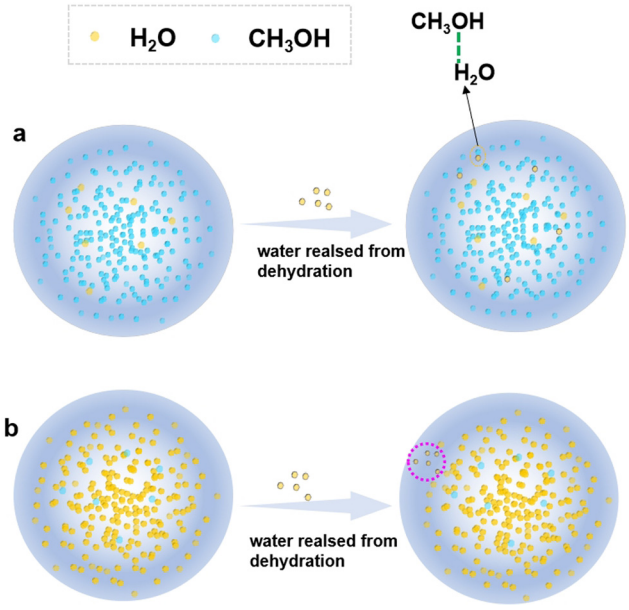

Figure 8: Diagrammatic sketch of methanol dehydration.

Figure 8b presents the influence of the mass of CH_3OH on the dehydration. When there is excessive CH_3OH in the reaction system, the released water is quickly absorbed by CH_3OH owing to the hydrogen bonding, which is in favor of the removal of water and promotes the generation of CuO. When there is very little CH_3OH and excessive water in the reaction system, where the CH_3OH has been previously combined with water by hydrogen bonding; thus, it was unfavorable to the dehydration of $Cu(OH)_4^{2-}$ in step III. In addition, according to the basic principles of chemistry, the excessive of free water in the reaction was detrimental to the equilibrium reaction to move right, thus restricting the generation of CuO. This can reasonably explain why it took a much longer time (at least 3 h) for Zhao and Zhao to obtain nano-CuO particles; they only used water as the solvent of $CuSO_4$ [31].

3.4 Recovery of CH_3OH and cycle preparation of nano-CuO

There are four components, including CuO, Na_2SO_4, CH_3OH, and water, that existed in the solution after the reaction. This raises an issue on the separation of the by-product Na_2SO_4 and the recycling of the solvent, or else it does not meet the principle of sustainable development. Therefore, a green sustainable route for the cyclic utilization of solvent was designed as described in the experiment part: the as-prepared CuO and the by-product Na_2SO_4 were separated successively from the solution by a physic filtration followed by a high-speed centrifugation so that the recovery of CH_3OH/water solution was realized.

Commonly, Na_2SO_4 exists in water in the form of Na^+ and SO_4^{2-} (Figure 9a), while in the CH_3OH/water solution, Na^+ and SO_4^{2-} tend to form Na_2SO_4 because it has very low solubility in CH_3OH (Figure 9b). At the function of high-speed centrifugation, Na_2SO_4 molecules were forced to move to the outside of the CH_3OH/water solution interface quickly (Figure 9c) and deposited on the bottom of the tube (Figure 9d). The XRD result further proved that the white deposited powders are Na_2SO_4 (Figure S6). In addition, barium chloride was added into the supernate, there was no precipitate formed in the supernate, which proved that the Na_2SO_4 had been completely removed.

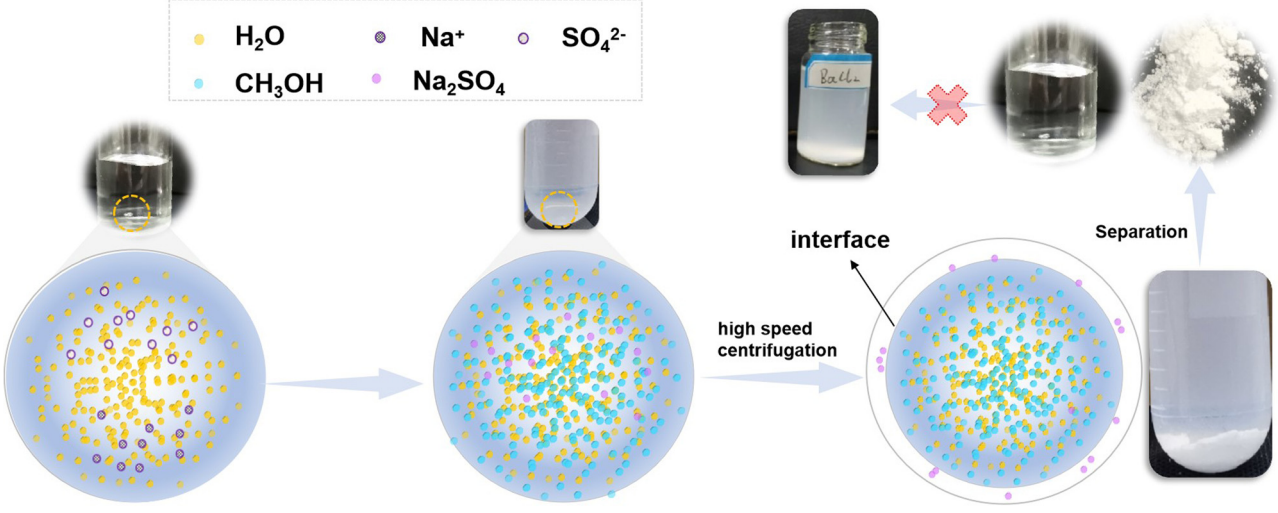

Figure 9: Diagrammatic sketch of separation of the by-product Na_2SO_4 under high-speed centrifugation.

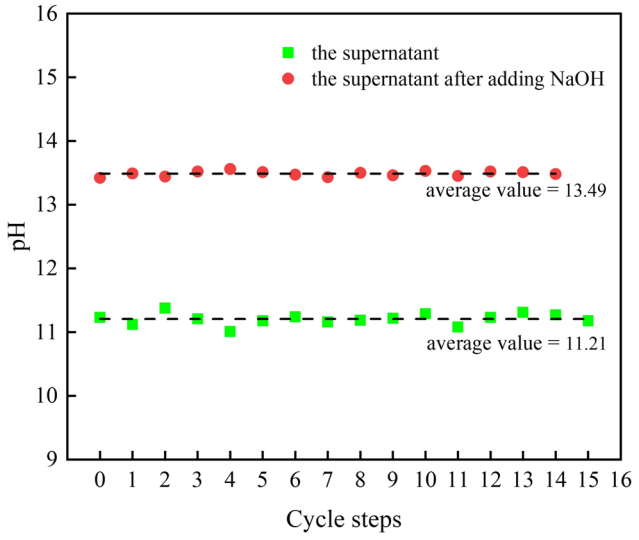

Figure 10: Solution pH in each preparation step.

In this case, the by-product Na_2SO_4 could be removed in 5 min by high-speed centrifugation with a total power of 700 kW/h. The energy consumption is around 225 kJ, which is a little higher than that of the traditional evaporation method to remove the water and methanol (202.66 kJ). The detailed calculation of the energy consumption for evaporation is shown in SI. Considering that the high-speed centrifugation can save more time and is more convenient to operate compared to evaporation, therefore, high-speed centrifugation was adopted to recover methanol in this work.

Before the first reaction, the CH_3OH/NaOH solution had an initial pH value of 13.68. Normally, the solution should be neutral at the end of the reaction of an equivalent amount of NaOH and $CuSO_4$. However, it can be seen from Figure 10 and Table S1 that at the end of each circulation, the pH value of the supernate fluctuated around 11.2, referring that there was plenty of OH^- in the solution and could be the most definitive evidence for the transformation of $Cu(OH)_4^{2-}$ to CuO (step III). Moreover, the high pH value, as well as the transparent color, also infers that there is no copper ion (Cu^{2+}) in the solution. To ensure the reproducibility of the result, a fixed mass of 1.8 g NaOH was added before the circle so that the pH value increased to about 13.5 again (Figure 10).

In all, the CH_3OH aqueous solution was reused 15 times in this work. TEM (Figure 11, Figure S7) and XRD tests were conducted to explore the physicochemical properties of the as-prepared CuO in each round. TEM results show that the CuO particles prepared in the first three rounds of recycling have a regular size with a length and thickness of about 20 and 5 nm, respectively (Figure 11a–c), which is similar to that of the initial sample as shown in Figure 6. With the increase in cycle rounds, the length of the as-

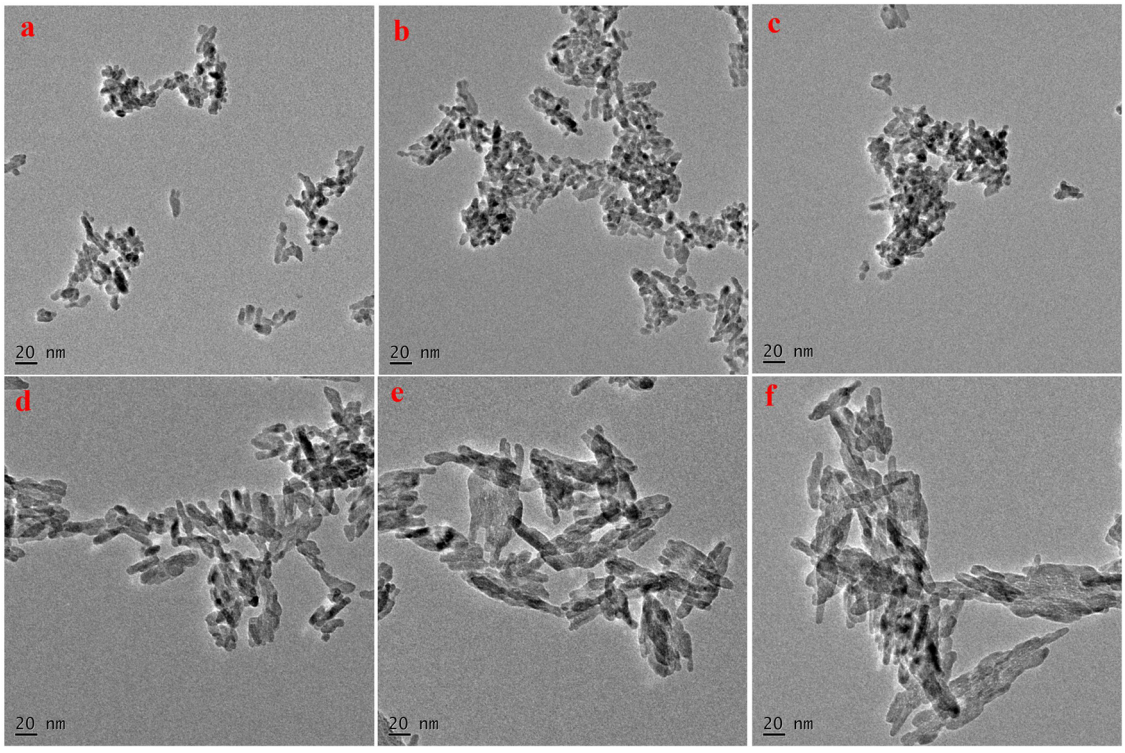

Figure 11: TEM morphologies of cycle-prepared nano-CuO.

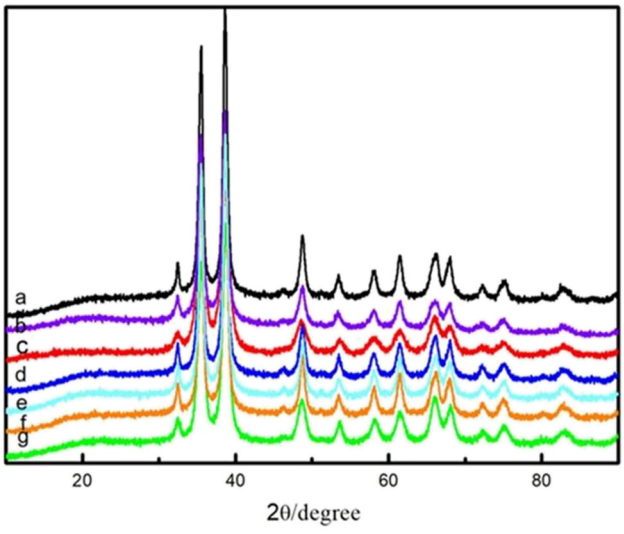

Figure 12: XRD pattern: (a) CuO prepared at the first time and (b–g) CuO obtained in the 1st, 2nd, 4th, 7th, 11th, and 14th cycles.

prepared CuO particles gradually increased from 20 to 50 nm. Accordingly, the thickness of the particles increased to 10 nm (Figure 11d–f). The results implied that the as-prepared particles still retained nanoscale size and integrity with the circulation of methanol, which guaranteed the realization of the reuse of methanol so that it has great meaning of resource environmental protection.

The XRD spectra of the seven selected CuO samples are shown in Figure 12. The peak position, as well as the shape of the 2θ for the selected samples, is identical to each other. The 2θ locates at 32.5°, 35.6°, 38.8°, 48.8°, 61.6°, and 83.1° and is assigned to the (110), (−111), (111), (−202), (−113), and (222) crystal planes, respectively, which is in perfect agreement with the CuO standard map card (JCPDS file: 72-0629). The above results refer that the CH_3OH solution can be reused and has little effect on the physical properties of the as-prepared CuO.

During the separation process, a trace loss of wet nano-CuO powders was inevitable because they tended to stick to the paper filter, thus leading to a lower yield of CuO compared to the theoretical calculated value (0.02 mol, equivalent to 1.5909 g). As shown in Table 1, it is clear to see that the average yield of CuO is about 1.5508 g, which is equivalent to about 97.5% of the theoretical value of 1.5909 g. The XPS patterns of the selected samples (1st, 2nd, 4th, 7th, 11th, and 14th) are very similar to that of Figure 2. The data shown in Table 1 also prove that the as-prepared CuO is able to adsorb CH_3OH during preparation. The average adsorption amount of CH_3OH reached 0.0146 g. This value gradually increased to 0.1068 g if we did not separate the as-prepared CuO from the clear liquid in time.

3.5 Antibacterial performance and spinnability of PA6-CuO composites

Most published literature has disclosed that CuO had a positive impact in improving the antibacterial performance of

Table 1: The mass of CuO obtained at each round

Cycle round	M_{CuO} after WD washing (g)	M_{CuO} after washing with ether (g)	Adsorbed methanol (g)	Percentage of methanol adsorbed (%)	Yield of CuO (%)
1st preparation	1.6151	1.5566	0.0585	3.62	97.84
The 1st cycle	1.6132	1.5405	0.0727	4.51	96.83
The 2nd cycle	1.6356	1.5389	0.0967	5.91	96.73
The 3rd cycle	1.6689	1.5621	0.1068	6.40	98.19
The 4th cycle	1.5801	1.5432	0.0369	2.34	97.00
The 5th cycle	1.6490	1.5725	0.0765	4.64	98.84
The 6th cycle	1.6115	1.5738	0.0377	2.34	98.93
The 7th cycle	1.6085	1.5468	0.0617	3.84	97.23
The 8th cycle	1.5740	1.5386	0.0354	2.25	96.71
The 9th cycle	1.5674	1.5479	0.0195	1.24	97.30
The 10th cycle	1.5811	1.5502	0.0309	1.95	97.44
The 11th cycle	1.6008	1.5259	0.0749	4.68	95.91
The 12th cycle	1.5788	1.5642	0.0146	0.92	98.32
The 13th cycle	1.6444	1.5527	0.0917	5.58	97.60
The 14th cycle	1.6090	1.5645	0.0445	2.77	98.34
The 15th cycle	1.5985	1.5351	0.0634	3.97	96.49
Average value	1.6085	1.5508	0.0577	3.56	97.48
Standard deviation	0.0293	0.0139	0.0277	1.6634	0.8716

polymer. Considering that, in recent years, the commercial demand for antibacterial PA6 fiber composite materials has developed fast [35–37], thereby, the antibacterial performance of the as-prepared nano-CuO in PA6 polymer was especially evaluated according to the national standard GB/T 20944.3 2008. Figure 13a indicates that pure PA6 was easy to be contaminated by bacteria; *E. coli* and *S. aureus* in the discs grew confluently so that the number of bacteria was countless. As the adding content of CuO increased to 0.12 wt%, the reproduction of *S. aureus* and *E. coli* was significantly inhibited and the numbers decreased to less than 106 and 30, respectively (Figure 13b). The results also prove that the antibacterial performance of the as-prepared CuO against *E. coli* is more effective than that of *S. aureus*, this is because the Gram-positive bacteria have a thicker cell wall than that of Gram-negative, so the Cu^{2+} provides stronger antibacterial activity on *E. coli* [38–40]. Gladly, the bactericidal rate of the PA6-CuO composite reached 100% when added 0.24 wt% Cu^{2+}; there was no living colony in the disc. It infers that by adding a tiny amount of the as-prepared nano-CuO into PA6 polymer, the released Cu^{2+} is enough to kill all bacterium, thus effectively saving the dosing of the antibacterial agent, which is highly similar to our previous work [37].

The spinnability of composite is a key feature to evaluate whether it is suitable to produce fiber composite or not. In this work, the PA6-CuO was further spun at a speed of 800 m/min, with a drawing ratio of 3.5. As shown in Figure 13c, the surface of PA6-CuO fiber appeared highly smooth under a scanning electron microscope. There was not any aggregated particle article being found even when adding 1 wt% CuO which far exceeds the minimum adding content of CuO which meets the antibacterial requirement. What is more, the fibers produced under a drawing ratio of 3.5 showed an average diameter of 27.44 μm. The smooth and regular morphology of PA6-CuO fiber clearly infers that the nano-CuO is highly compatible with the PA6 matrix and has good spinnability superior to that of

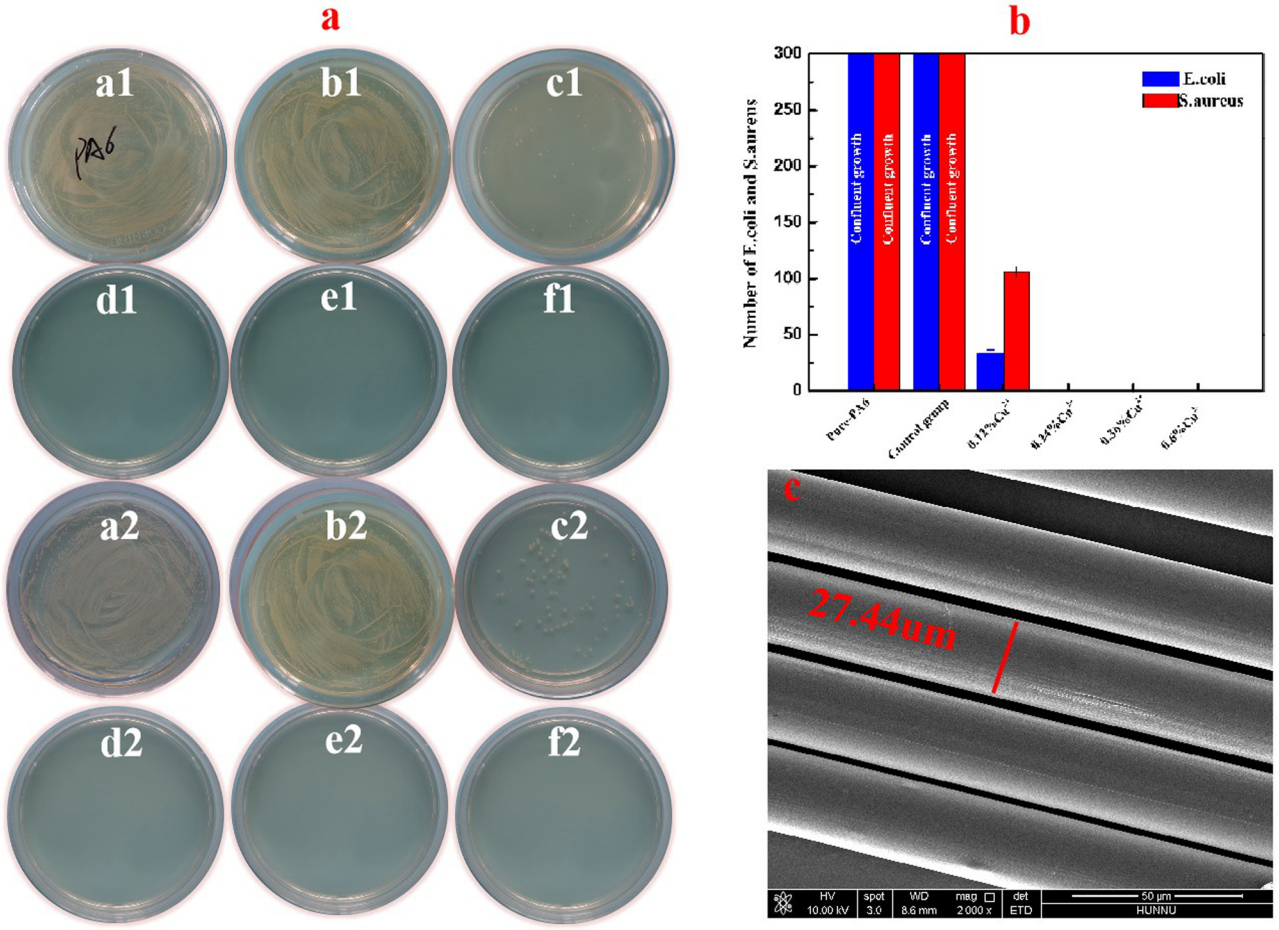

Figure 13: Antibacterial performance of PA6-CuO composites with different copper contents: (a–f) Cu^{2+} containing 0 (pure PA6), 0 (control group), 0.12, 0.24, 0.36, and 0.6 wt%, respectively; (b) bacterial number; and (c) spinnability of fiber size.

reported results [28,41]. Besides, the refraction and the reflection of light were changed by the addition of nano-CuO, thus inducing variable optical effects on the fiber composite; as a result, the manufactured fibers appear silvery-white rather than the expected black. To sum up, the PA6-CuO composite has good spinnability when producing fine silk through a continuous spinning process and gives the fiber materials superior antibacterial properties, which implies that it has a potential application in the field of the fiber industry.

4 Conclusions

In this work, by simply adding dropwise $CuSO_4$ aqueous solution into $NaOH/CH_3OH$ solution at room temperatures (0–30°C), CuO nanoparticles with a controllable size were obtained in 25 min. The average length and thickness of the particles are around 20 and 5 nm, respectively. More importantly, agent methanol could accelerate the dehydration of the $Cu(OH)_4^{2-}$ intermediate to produce CuO during the reaction, which significantly reduced the reaction time compared to the conventional method, and effectively increased the average yield rate of CuO to 97.48%. What is more, methanol was proved to be in favor of the separation of the by-products Na_2SO_4 from the aqueous solution by high-speed centrifugation, which allowed the recycling of the CH_3OH aqueous solution to be realized. Thereby, an environmentally friendly sustainable route for preparing nano-CuO at room temperatures was proposed. Additionally, the as-prepared CuO presented a superior antibacterial performance in PA6-CuO fiber composites. By adding only 0.24 wt% CuO, the antibacterial rate of the composites reached 100% for both *E. coli* and *S. aureus*. We believe that this sustainable one-pot synthesis method can be further extended to synthesize CuO-based nanocoprecipitates with multifunction. However, the reason for the absorption of CH_3OH by CuO needs to be evaluated in detail in the future.

Acknowledgments: The authors acknowledge the support of the Open Foundation of National & Local Joint Engineering Laboratory for New Petro-chemical Materials and Fine Utilization of Resources (grant number KF201804), Hunan Normal University, and the Open Fund of State Key Laboratory of Biobased Fiber Manufacturing Technology (grant number SKL202210), China Textile Academy. Special thanks to Prof. Xiaoyi Yi (Central South University, China) for guidance to remove the methanol by ether wash.

Funding information: This research was supported by the Open Foundation of National & Local Joint Engineering Laboratory for New Petro-chemical Materials and Fine Utilization of Resources (grant number KF201804), Hunan Normal University, and the Open Fund of State Key Laboratory of Biobased Fiber Manufacturing Technology (grant number SKL202210), China Textile Academy.

Author contributions: Yongseng Niu: experiments, methodology, writing – original draft, Boren Xu: experiments, measurements; Xin Yi: experiments; Xi Wang: supervision, investigation, reviewing and editing; Chunwang Yi: supervision, investigation, reviewing and correcting the draft, writing point to point response. All authors have accepted responsibility for the entire content of this manuscript and approved its submission.

Conflict of interest: The authors state no conflict of interest.

Data availability statement: All data generated or analyzed during this study are included in this published article.

References

[1] Porkovich A, Ziadi Z, Kumar P, Kioseoglou J, Jian N, Weng L, et al. In situ observation of metal to metal oxide progression: A study of charge transfer phenomenon at Ru–CuO interfaces. ACS Nano. 2019;13:12425–37.

[2] Guo A, Zhou Q, Bao Y, Qian F, Zhou X. Prochloraz alone or in combination with nano-CuO promotes the conjugative transfer of antibiotic resistance genes between Escherichia coli in pure water. J Hazard Mater. 2020;424:127761.

[3] Naseer A, Ali S, Haider W. Powder injection molded nano copper oxide grafted graphene reinforced copper matrix composites. Powder Technol. 2022;397:117101.

[4] Mazurkow JM, Yuzbasi NS, Domagala KW, Pfeiffer S, Kata D, Graule T. Nano-sized copper (Oxide) on alumina granules for water filtration: Effect of copper oxidation state on virus removal performance. Env Sci Technol. 2019;54:1214–22.

[5] Zhang Q, Zhang K, Xu D, Yang G, Huang H, Nie F, et al. CuO nanostructures: Synthesis, characterization, growth mechanisms, fundamental properties, and applications. Prog Mater Sci. 2014;60:208–337.

[6] Seo SD, Jin YH, Lee SH, Shim HW, Kim DW. Low-temperature synthesis of CuO-interlaced nanodiscs for lithium ion battery electrodes. Nanoscale Res Lett. 2011;6:397.

[7] Bu YYI. Novel all solution processed heterojunction using p-type cupric oxide and n-type zinc oxide nanowires for solar cell applications. Ceram Int. 2013;39:8073–8.

[8] Naatz H, Lin S, Li R, Jiang W, Ji Z, Chang CH, et al. Safe-by-design CuO nanoparticles via Fe-doping, Cu–O bond length variation, and

biological assessment in cells and zebrafish embryos. ACS Nano. 2017;11:501–15.
[9] Duan Y, Liu X, Han L, Asahina S, Xu D, Cao Y, et al. Optically active chiral CuO “nanoflowers”. J Am Chem Soc. 2014;136:7193–6.
[10] Liu Y, Liu X, Qiu K, Cheng J, Wang W, Yan H, et al. Facile synthesis of graphene-like copper oxide nanofilms with enhanced electrochemical and photocatalytic properties in energy and environmental applications. ACS Appl Mater Inter. 2015;7:9682–90.
[11] Paglia F, Vak D, Van Embden J. Photonic sintering of copper through the controlled reduction of printed CuO nanocrystals. ACS Appl Mater Inter. 2015;7:25473–8.
[12] Perelshtein I, Applerot G, Perkas N. CuO-cotton nanocomposite: Formation, morphology, and antibacterial activity. Surf Coat Tech. 2009;204:54–7.
[13] Wang H, Xu JZ, Zhu JJ, Chen HY. Preparation of CuO nanoparticles by microwave irradiation. J Cryst Growth. 2002;244:88–94.
[14] Lin XZ, Liu P, Yu JM. Synthesis of CuO nanocrystals and sequential assembly of nanostructures with shape-dependent optical absorption upon laser ablation in liquid. J Phys Chem C. 2009;113:17543–7.
[15] Yin M, Wu CK, Lou YB. Copper oxide nanocrystals. J Am Chem Soc. 2005;127:9506–11.
[16] Pfeifer P, Schubert K, Emig G. Preparation of copper catalyst washcoats for methanol steam reforming in microchannels based on nanoparticles. Appl Catal A-Gen. 2005;286:175–85.
[17] Bouzit SE, Boualy B, Firdoussi L. Fast room temperature solution-phase approach for selective synthesis of nanostructured $Cu(OH)_2$, Cu_2O and CuO. Int Res J Pure Appl Chem. 2015;8:157–64.
[18] Hu M, He J, Yang M. Controlled synthesis of nanostructured copper oxides through an elaborate solution route. J Nanosci Nanotechnol. 2016;16:783.
[19] Dar MA, Ahsanulhaq Q, Kim YS, Sohn JM, Kim WB, Shin HS. Versatile synthesis of rectangular shaped nanobat-like CuO nanostructures by hydrothermal method; structural properties and growth mechanism. Appl Surf Sci. 2009;255:6279–84.
[20] Zhuang Z, Peng Q, Li Y. Controlled synthesis of semiconductor nanostructures in the liquid phase. Chem Soc Rev. 2011;40:5492–513.
[21] Ozga M, Kaszewski J, Seweryn A, Sybilski P, Godlewski M, Witkowski BS. Ultra-fast growth of copper oxide (II) thin films using hydrothermal method. Mat Sci Semicon Proc. 2020;120:105279.
[22] Chauhan D, Satsangi VR, Dass S. Preparation and characterization of nanostructured CuO thin films for photoelectrochemical splitting of water. Bull Mater Sci. 2006;29(7):709–16.
[23] Kim DS, Kim JC, Kim BK. One-pot low-temperature sonochemical synthesis of CuO nanostructures and their electrochemical properties. Ceram Int. 2016;42:19454–60.
[24] Chen TW, Rajaji U, Chen SM. Facile synthesis of copper(II) oxide nanospheres covered on functionalized multiwalled carbon nanotubes modified electrode as rapid electrochemical sensing platform for super-sensitive detection of antibiotic. Ultrason Sonochem. 2019;58:104596.
[25] Saadatian MH, Shahverdizadeh GH, Babazadeh M, Edjlali L, Es’haghi M. The effect of ultrasonic irradiation power and initial concentration on the particle size of nano copper(II) coordination polymer: Precursors for preparation of CuO nanostructures. J Polym Res. 2022;29:57.
[26] Zhu HT, Zhang CY, Tang YM, Wang JX. Novel synthesis and thermal conductivity of CuO Nanofluid. J Phys Chem C. 2007;111:1646–50.
[27] Amaniampong PN, Trinh QT, Varghese JJ. Unraveling the mechanism of the oxidation of glycerol to dicarboxylic acids over a sonochemically synthesized copper oxide catalyst. Green Chem. 2018;20:2730–41.
[28] Lu C, Qi L, Yang J. Simple template-free solution route for the controlled synthesis of $Cu(OH)_2$ and CuO nanostructures. J Phys Chem B. 2004;108:17825–31.
[29] Jia W, Reitz E, Sun H. From $Cu_2(OH)_3Cl$ to nanostructured sisal-like $Cu(OH)_2$ and CuO: Synthesis and characterization. J Appl Phys. 2009;105:064917.
[30] Cudennec Y, Lecerf A. The transformation of $Cu(OH)_2$ into CuO, revisited. Solid State Sci. 2003;5:1471–4.
[31] Zhao Y, Zhao J. Room temperature synthesis of 2D CuO nanoleaves in aqueous solution. Nanotechnology. 2011;22:115604.
[32] Francisco MSP, Mastelaro VR, Nascente PAP. Activity and characterization by XPS, HR-TEM, Raman spectroscopy, and BET surface area of CuO/CeO_2-TiO_2 catalysts. J Phys Chem B. 2001;105:10515–22.
[33] Chen YZ, Liaw BJ, Chen HC. Selective oxidation of CO in excess hydrogen over CuO/CexZr1-xO_2 catalysts. Int J Hydrog Energ. 2006;31:427–35.
[34] Sarkar D, Khan GG, Singh AK. High-performance pseudocapacitor electrodes based on α-Fe_2O_3/MnO_2 core–shell nanowire heterostructure arrays. J Phys Chem C. 2013;117:15523–31.
[35] Chen J, Gong CH, Yang C, Yi CW. Flexible preparation of polyamide-6 based thermoplastic elastomers via amide exchange. J Mater Sci. 2021;56:12018–29.
[36] Zhang YJ, Zheng W, Xiao YJ, Yi CW. Preparation of high-efficient flame retardant PA6 via DOPO-ITA initiated ring-opening polymerization of caprolactam. J Polym Sci. 2024;62:547–53.
[37] Xu BR, Yi CW. Preparation of nano-CuO@BaSO 4 under room temperatures and its application in PA6 composites. J Reinf Plast Comp. 2024. doi: 10.1177/07316844241236871.
[38] Pant HR, Pant DR, Pandeya G, Panthi KT, Nam ST, Hong CS, et al. Characterization andm antibacterial properties of Ag NPs loaded nylon-6 nanocomposite prepared by one-step electrospinning process. Colloid Surf A. 2012;395:94–9.
[39] Kara S, Ureyen ME, Erdogan UH. Structural and antibacterial properties of PP/CuO composite filaments having different cross sectional shapes. Int Polym Proc. 2016;31:398–409.
[40] Ahmad MM, Kot HM, Mushtaq S, Waheed-Ur-Rehman M, Maghanga CM, Alam MW. Green synthesis of Mn + Cu bimetallic nanoparticles using Vinca rosea extract and their antioxidant, antibacterial, and catalytic activities. Crystals. 2022;12(1):72.
[41] Zhang W, Xu B, Gong C. Antibacterial and anti-flaming PA6 composite with metathetically prepared nano AgCl@ $BaSO_4$ co-precipitates. Front Chem Sci Eng 2021;15:340–50.